Pseudo-Lattice Treatment for Subspace Aligned Interference Signals

Yahya H. Ezzeldin and Karim G. Seddik, *Member, IEEE*

***Abstract*—In this paper, we propose a channel transformation technique for joint decoding of desired and interfering signals in an interference alignment scenario consisting of K users with multiple antennas. Our technique, i.e., pseudo-lattice treatment, is based on the compute-and-forward framework. Our technique can be implemented to provide decoding gains with low complexity for subspace aligned interference signals. We evaluate the performance of the system through simulations that show the performance gain attained by using our pseudo-lattice method over subspace decoding techniques for interference alignment in low- and medium-SNR conditions.**

***Index Terms*—Lattice interference alignment, lattice reduction, multiple-input–multiple-output (MIMO), subspace interference alignment.**

I. Introduction

Interference management is one of the key challenges for spectrum sharing in wireless communications. Different techniques for managing interference among users sharing the same frequency band have been developed in the literature. As a characterization of available communication resources, the number of degrees of freedom (DoF) is used to represent the interference-free dimensions in a communication network that can be shared between interfering users. For a two-user interference channel, different techniques can be used to achieve half of the DoF per user, through time division or spatial multiplexing, etc.

If we scale the problem to a K-user interference network, the aforementioned solutions can achieve as much as $1/K$ of the DoF per user. In [1], *interference alignment* is proposed as a strategy for handling interference in multiuser interference networks and is shown to achieve 1/2 DoF per user, independent of the number of users in the network. The technique used precoded signals transmitted from each of the K transmitters such that, for each receiver, the $K-1$ interfering signals are collinear and can therefore be modeled as a single interference source. Therefore, the problem simplifies to a two-user interference network problem, and the desired signal can be decoded using local channel information at each receiver through zero forcing (ZF). In [2], the feasibility of interference alignment for a multiple-input–multiple-output (MIMO) interference channel is investigated and shown to exhibit performance gains over other interference management techniques using a distributed framework.

Applying structured lattice codes to study the capacity of interference alignment over the signal scale instead of signal space is introduced in [3], where they study the theoretic capacity of the many-to-one interference channel using the deterministic channel model. The achievable region for the three-user Gaussian interference channel is studied in [4] when applying a layered lattice coding transmission strategy for interference alignment. The feasibility of applying lattice interference alignment (L-IA) for a MIMO interference channel is studied in [5]. It is shown that the use of low-complexity lattice reduction (LR) decoders [6], [7] at the receivers can substantially improve the decoding performance while maintaining low complexity. The work also explains that the application of the aforementioned technique in a three-user network is limited to two users, whereas the third user is not able to benefit from the lattice interference alignment.

In this paper, we propose a low-complexity decoder for signal-space interference alignment in a MIMO three-user interference network. Our decoder achieves suboptimal performance with reduced complexity for signal-space interference alignment. Optimal results for signal-space aligned interference signals can be performed using maximum likelihood (ML) decoders at the cost of high complexity, which is even more critical for systems with higher signal dimensions. Therefore, we propose a *pseudo-lattice treatment* that allows usage of LR-based decoders in scenarios where lattice interference alignment is not applicable to all users. Our treatment can be used in subspace interference alignment (S-IA) for all users or in L-IA to overcome the aforementioned implementation limitation presented in [5] for all users. In the case in which L-IA is achieved by the transmitters, our decoder performs on par with the ML decoder. It is worth noting that the pseudo-lattice decoder requires no further coordination between the transmitters than what S-IA or L-IA requires; the channel transformation to enforce lattice-structured interference is performed locally by the receiver, as we shall explain further in this paper. Our technique uses compute-and-forward (C&F) relaying technique [8] as its core to calculate a linear combination of the transformed lattice structures. In [9], signal-scale interference alignment is performed by applying C&F with asymmetric power allocation. Our "pseudo-lattice" technique is built on top of signal-space interference alignment; therefore, power allocation is limited per transmitter unlike the aforementioned work.

The remainder of this paper is organized as follows. In Section II, we introduce the model for our MIMO multiuser interference channel. In Section III, we discuss basic interference alignment schemes and the difference between our proposed treatment and the discussed schemes. Finally, in Section IV, we present a mathematical analysis of the performance of the receiver in terms of decoding error probability when our framework is implemented. Then, we discuss different examples of how the channel transformation treatment can be implemented and how the system performs under these different implementations. Finally, in Section V, we present simulation results and then follow with conclusions on the work presented in this paper.

Notations: Throughout this paper, we use $\mathbb{Z}$ to refer to real integers and $\mathbb{C}$ to refer to the field of complex numbers. We represent vectors in bold lowercase letters such as $\mathbf{x} \in \mathbb{C}^N$. Matrices are represented by bold uppercase letters such as $\mathbf{A} \in \mathbb{C}^{M \times N}$. The superscripts T and H denote the transpose and Hermitian transpose of a matrix, respectively. The ℓ_2-norm of vector $\mathbf{a}$ is denoted $\|\mathbf{a}\|$. $\mathbf{A}^\dagger$ and $\|\mathbf{A}\|$ denote the pseudoinverse and Frobenius norm of matrix $\mathbf{A}$, respectively.

II. System Model

We consider an interference network with three transmitter–receiver pairs each equipped with $N > 1$ antennas. The ith transmitter generates a single message signal $\mathbf{w}_i \in \mathbb{C}^{\lfloor N/2 \rfloor}$ to be transmitted through the interference channel and intended for receiver i. The messages are linearly precoded before transmission using $\mathbf{B}_i \in \mathbb{C}^{N \times \lfloor N/2 \rfloor}$ and

Manuscript received August 20, 2013; revised December 17, 2013 and March 4, 2014; accepted April 4, 2014. Date of publication April 16, 2014; date of current version November 6, 2014. The review of this paper was coordinated by Prof. S.-H. Leung.

Y. H. Ezzeldin is with the Department of Electrical Engineering, Alexandria University, Alexandria 2156, Egypt (e-mail: yahya.ezzeldin@ieee.org).

K. G. Seddik is with the Department of Electronics Engineering, The American University in Cairo, New Cairo 11835, Egypt (e-mail: kseddik@aucegypt.edu).

Color versions of one or more of the figures in this paper are available online at http://ieeexplore.ieee.org.

Digital Object Identifier 10.1109/TVT.2014.2317753

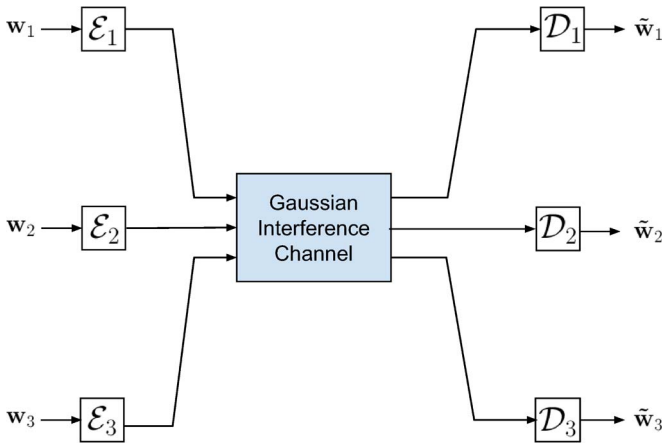

Fig. 1. System model for a three-user interference alignment network.

transmitted through a Gaussian interference channel as shown in Fig. 1. The received signal at receiver i is

$$\mathbf{r}_i = \sum_{j=1}^{3} \mathbf{H}_{i,\,j}\mathbf{B}_j\mathbf{w}_j + \mathbf{z}_i \tag{1}$$

where $\mathbf{H}_{i,\,j}$ denotes the $N \times N$ channel matrix between transmitter j and receiver i. The channel coefficients in $\mathbf{H}_{i,\,j}$ are independent identically distributed (i.i.d.) complex Gaussian channels with zero mean and variance σ^2. $\mathbf{z}_i$ is the background additive white Gaussian noise (AWGN) at receiver i, such that $\mathbf{z}_i \sim \mathcal{CN}\ (0,\, \sigma_z^2)$. The transmitted message signals $\mathbf{w}_i$ are drawn from a finite lattice constellation (e.g., quadrature-amplitude-modulated (QAM) constellations). These messages are subsequently encoded before the transmission. The block $\mathcal{E}_i$ in Fig. 1 represents the precoder at the ith transmitter. The output precoded signal is of normalized power P_s such that $\mathbb{E}\{\,\|\mathbf{B}_i\mathbf{w}_i\|_2^2\,\} = P_s$ for all i. The block $\mathcal{D}_i$ in Fig. 1 represents the decoder at the ith receiver node. The channel coefficients $\mathbf{H}_{i,\,j}$ are assumed perfectly known at the transmitters and receivers.

Lattice Structures at Transmitter and Receiver: In our model, we consider that the signals transmitted have a lattice constellation. Lattice $\mathcal{L}(\mathbf{G})$ represents the lattice generated using the *generator matrix* $\mathbf{G}$, i.e.,

$$\mathcal{L}(\mathbf{G}) = \left\{\mathbf{G}\mathbf{x} | \mathbf{x} \in \mathbb{Z}^{\lfloor N/2 \rfloor} + j\mathbb{Z}^{\lfloor N/2 \rfloor}\right\} = \mathbf{\Lambda}_G. \tag{2}$$

If we consider that lattice $\mathcal{L}(\mathbf{G}) \in \mathbb{C}^{\lfloor N/2 \rfloor}$ is transmitted from each of the three users, then the received signal is a superposition of several lattices. Generally, the received signal has no lattice structure as the channel coefficients can take noninteger values. In systems where the received signals have a lattice structure, the ML decoder or LR can be used to decode the original signal $\mathbf{x}$. We define the *Voronoi region* $\mathcal{V}_\Lambda(\boldsymbol{\lambda})$ as the set of points that are closer to $\boldsymbol{\lambda} \in \mathbf{\Lambda}$ than any other point in the lattice $\mathbf{\Lambda}$. An ML decoder would map the points in this region to the center of the Voronoi region. Similarly, in the LR algorithms, the incentive is also to map $\mathcal{V}_\Lambda(\boldsymbol{\lambda})$ to the nearest lattice point but with lower complexity.

In the following, we discuss the different techniques for interference alignment that lead up to our pseudo-lattice treatment.

III. Interference Alignment and Proposed Framework

At receiver i, the signal in (1) contains the desired message component $\mathbf{H}_{i,\,i}\mathbf{B}_i\mathbf{w}_i$ and interference components $\sum_{j\neq i} \mathbf{H}_{i,\,j}\mathbf{B}_j\mathbf{w}_j$. Using interference alignment [2], we can set the interfering signals to be approximately collinear at the receiver. As a result, the collective interference can be regarded as a single interference source, confining the interference to an $\lfloor N/2 \rfloor$ subspace. The nominal interference alignment setting is to decode when the interference is aligned in a subspace of the signal space.

A. Subspace Interference Alignment

In S-IA, interference alignment is performed in the signal space. The transmitter precoders limit the interference received at the receiver to a subspace of $\lfloor N/2 \rfloor$ (not necessarily orthogonal with the desired signal subspace). For a three-user system, the condition for aligning interference at receiver 1 can be expressed as

$$\text{span}(\mathbf{H}_{1,\,2}\mathbf{B}_2) = \text{span}(\mathbf{H}_{1,\,3}\mathbf{B}_3). \tag{3}$$

Decoding of the desired signal can be performed using the conventional ZF decoder. For example, decoding for user 1 is as follows:

$$\left[\tilde{\mathbf{w}}_\mathbf{1}^T\ \tilde{\mathbf{w}}_{\text{int}}^T\right]^T = \left[\mathbf{H}_{1,\,1}\mathbf{B}_1\ \mathbf{H}_{1,\,2}\mathbf{B}_2\right]^\dagger \mathbf{r}_1.$$

B. Lattice Interference Alignment

In L-IA, alignment takes place in both the signal-space and signal-scale. In [5], a framework for aligning lattice structures instead of spaces have been introduced for a three-user system. In this framework, users aim to match their respective lattice generating functions such that

$$\mathcal{L}(\mathbf{H}_{1,\,2}\mathbf{B}_2) = \mathcal{L}(\mathbf{H}_{1,\,3}\mathbf{B}_3) \tag{4}$$

$$\mathcal{L}(\mathbf{H}_{2,\,1}\mathbf{B}_1) = \mathcal{L}(\mathbf{H}_{2,\,3}\mathbf{B}_3) \tag{5}$$

$$\mathcal{L}(\mathbf{H}_{3,\,1}\mathbf{B}_1) = \mathcal{L}(\mathbf{H}_{3,\,2}\mathbf{B}_2) \tag{6}$$

where $\mathcal{L}(\mathbf{G})$ represents the lattice generated using the *generator matrix* $\mathbf{G}$, (i.e., $\mathcal{L}(\mathbf{G}) = \{\mathbf{G}\mathbf{x} \mid \mathbf{x} \in \mathbb{Z}^{\lfloor N/2 \rfloor} + j\mathbb{Z}^{\lfloor N/2 \rfloor}\}$). As Choi discusses in [5], these conditions cannot be met for interference at each of the receivers, and signal-scale alignment is only achieved for two of the receivers. For the remaining receiver, only S-IA is achievable, and ZF is applied to decode the desired signal for that receiver. (See [5] for further comparison between the performance of the two previously mentioned methods.)

C. Pseudo-Lattice Treatment

In this paper, we consider pseudo-lattice treatment for subspace aligned interference signals. As previously mentioned, a benefit of the signal to be decoded having a lattice structure is that we can apply low-complexity LR algorithms to decode the desired message $\mathbf{w}_i$ and the effective interference aligned signals.

We will discuss a three-user interference system as a representative to a K-user system. Assuming that subspace alignment is achieved at user 1, then the precoders are designed such that (3) is satisfied. The interference terms from user 2 and user 3 are now aligned in a subspace that can be expressed as the column space of $\mathbf{H}_{1,\,2}\mathbf{B}_2$ or $\mathbf{H}_{1,\,3}\mathbf{B}_3$. Although the interference is subspace aligned, it does not exhibit a lattice structure, although individual interference sources still retain their lattice structure. We denote $\mathbf{\Lambda}_2$ and $\mathbf{\Lambda}_3$ as the lattice received as interference from users 2 and 3, respectively. $\mathbf{\Lambda}_2$ and $\mathbf{\Lambda}_3$ can be expressed as

$$\begin{aligned}\mathbf{\Lambda}_2 &= \mathcal{L}(\mathbf{H}_{1,\,2}\mathbf{B}_2)\\ \mathbf{\Lambda}_3 &= \mathcal{L}(\mathbf{H}_{1,\,3}\mathbf{B}_3).\end{aligned} \tag{7}$$

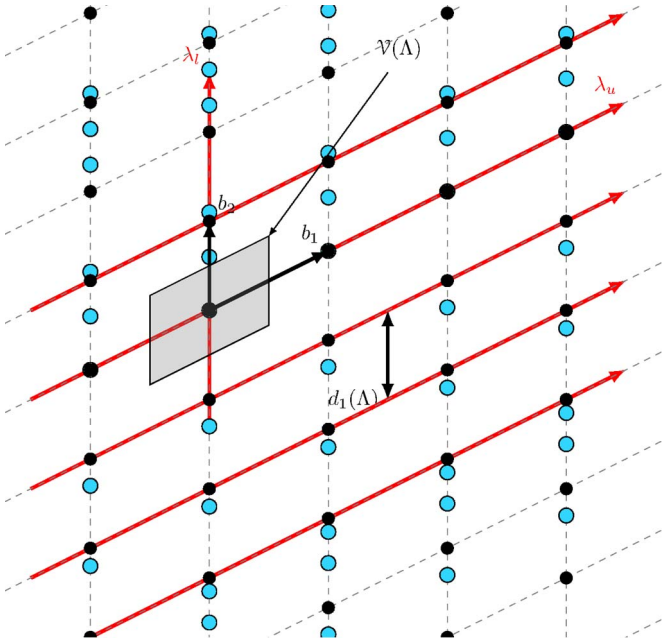

Fig. 2. Structure of the received signal in pseudo-lattice interference alignment. Lattice $\mathbf{\Lambda}_i$ at user i with the desired signal aligned in the direction of the basis b_1, the interference aligned in the direction of the basis b_2, and the number of antennas $N = 2$. The nonlattice structure of the interference signal is shown in blue, whereas the approximated structure is shown in black.

Although $\mathbf{\Lambda}_2$ and $\mathbf{\Lambda}_3$ are lattices, $\mathbf{\Lambda}_2 + \mathbf{\Lambda}_3$ is not generally a lattice. This is because $\mathbf{\Lambda}_2 \nsubseteq \mathbf{\Lambda}_3$ and $\mathbf{\Lambda}_3 \nsubseteq \mathbf{\Lambda}_2$; therefore, there is no ordered structure in the received signal. We can rewrite the expressions in (7) in terms of a common factor as follows:

$$\begin{aligned}\mathbf{\Lambda}_2 &= \mathcal{L}(\mathbf{H}_c\mathbf{D}_2)\\ \mathbf{\Lambda}_3 &= \mathcal{L}(\mathbf{H}_c\mathbf{D}_3).\end{aligned} \tag{8}$$

The expressions in (8) represent a redefinition of the interference subspace in terms of new basis $\mathbf{H}_c\mathbf{D}_j$, such that $\mathbf{D}_j = \mathbf{H}_c^{\dagger}\,\mathbf{H}_{1,j}\mathbf{B}_j \in \mathbb{C}^{N\times\lfloor N/2\rfloor}$. For $\mathbf{\Lambda}_2$ and $\mathbf{\Lambda}_3$ to be part of a larger lattice structure $\mathcal{L}(\mathbf{H}_c)$, $\mathbf{D}_2$, and $\mathbf{D}_3$ need to belong to $\mathbb{Z}^{N\times\lfloor N/2\rfloor} + j\mathbb{Z}^{N\times\lfloor N/2\rfloor}$. Finding $\mathbf{D}_2$ and $\mathbf{D}_3$ with complex integer terms such that $\mathbf{\Lambda}_2 \subseteq \mathbf{\Lambda}_3$ or $\mathbf{\Lambda}_3 \subseteq \mathbf{\Lambda}_2$ is not possible in most cases as previously mentioned. The matrices $\mathbf{D}_2$ and $\mathbf{D}_3$ are usually in complex terms, i.e., $\mathbb{C}^{N\times\lfloor N/2\rfloor}$, rather than complex integers. The received signal space therefore does not exhibit a lattice structure, as shown in Fig. 2.

We define $\varphi : \mathbb{C}^{N\times\lfloor N/2\rfloor} \longrightarrow \mathbb{Z}^{N\times\lfloor N/2\rfloor} + j\mathbb{Z}^{N\times\lfloor N/2\rfloor}$ as a surjective mapping function that maps matrix $\mathbf{A}$ to the nearest complex integer matrix $\varphi(\mathbf{A})$. The receiver can find groups of matrices $\{\mathbf{H}_c,\, \mathbf{D}_2,\, \mathbf{D}_3\}$ such that

$$\mathcal{L}\left(\mathbf{H}_c\,\varphi(\mathbf{D}_2)\right) \subseteq\ \mathcal{L}(\mathbf{H}_c), \quad \mathcal{L}\left(\mathbf{H}_c\,\varphi(\mathbf{D}_3)\right) \subseteq \mathcal{L}(\mathbf{H}_c). \tag{9}$$

The approximation in (9) introduces additional noise to the received signal. We can rewrite the interference signal from (1) as

$$\begin{aligned}\mathbf{r}_i &= \sum_{j=1}^{3}\mathbf{H}_{i,j}\mathbf{B}_j\mathbf{w}_j + \mathbf{z}_i = \mathbf{H}_{i,i}\mathbf{B}_i\mathbf{w}_i + \sum_{j\neq i}^{3}\mathbf{H}_c\mathbf{D}_j\mathbf{w}_j + \mathbf{z}_i\\ &= \underbrace{\mathbf{H}_{i,i}\mathbf{B}_i\mathbf{w}_i}_{\text{Desired Signal}} + \underbrace{\sum_{j\neq i}^{3}\mathbf{H}_c\,\varphi(\mathbf{D}_j)\mathbf{w}_j}_{\text{Lattice Interference}} + \underbrace{\sum_{j\neq i}^{3}\mathbf{H}_c(\mathbf{D}_j - \varphi(\mathbf{D}_j)\mathbf{w}_j}_{\text{Approximation noise}} + \mathbf{z}_i\\ &\qquad\qquad \underbrace{\qquad\qquad\qquad\qquad\qquad\qquad}_{\text{Effective noise}(\mathbf{n}_i)}\end{aligned}$$

where the effective noise $\mathbf{n}_i$ is the total noise seen by the LR decoder due to the background noise $\mathbf{z}_i$ and the noise introduced due to channel approximation. Note that, this is similar to the concept of lattice decoding of linear combinations in C&F relaying [8] and physical network coding in [10]. For our three-user system, the incentive is to find the matrix tuple $\{\mathbf{H}_c,\, \mathbf{D}_2,\, \mathbf{D}_3\}$, which minimizes the difference between the effective noise $\mathbf{n}_i$ and background noise $\mathbf{z}_i$, i.e.,

$$\{\mathbf{H}_c,\, \mathbf{D}_2,\, \mathbf{D}_3\} = \min_{\mathbf{H}_c,\,\mathbf{D}_2,\,\mathbf{D}_3}\left\|\sum_{j=2}^{3}\mathbf{H}_c\left(\mathbf{D}_j - \varphi(\mathbf{D}_j)\right)\right\|_F^2$$

such that :

$$\mathbf{H}_c\mathbf{D}_j = \mathbf{H}_{1,j}\mathbf{B}_j. \tag{10}$$

This is a receiver incentive; therefore, there is no disruption to S-IA or L-IA at other receivers as the precoding matrices are still calculated to satisfy the equation conditions discussed in Section III-A and B.

Choosing the matrix $\mathbf{H}_c$*:* As previously mentioned, for a three-user system, the target is to find the tuple $\{\mathbf{H}_c,\, \mathbf{D}_2,\, \mathbf{D}_3\}$ that satisfies (10). The Frobenius norm $\|\mathbf{A}\|_F^2$, where $\mathbf{A} \in \mathbb{C}^{N\times\lfloor N/2\rfloor}$, is the regular vector Euclidean norm when $\mathbf{A}$ is viewed as a vector with dimensions $(N^2/2)\times 1$. To evaluate problem (10), we can rewrite the problem as follows:

$$\begin{aligned}\{\mathbf{H}_c,\, \mathbf{D}_2,\, \mathbf{D}_3\} &= \left\{\mathbf{H}_c,\, \frac{\mathbf{H}_{1,2}\mathbf{B}_2}{\mathbf{H}_c},\, \frac{\mathbf{H}_{1,3}\mathbf{B}_3}{\mathbf{H}_c}\right\}\\ &= \min_{\mathbf{H}_c}\left\|\sum_{j=2}^{3}\mathbf{H}_{1,j}\mathbf{B}_j - \varphi\left(\frac{\mathbf{H}_{1,j}\mathbf{B}_j}{\mathbf{H}_c}\right)\right\|_F^2\\ &= \min_{\mathbf{H}_c}\left\|\sum_{j=2}^{3}c_j - \varphi\left(\frac{c_j}{\mathbf{H}_c}\right)\right\|_F^2.\end{aligned} \tag{11}$$

The problem in (11) is clearly not convex. Furthermore, we are performing our treatment based on channel knowledge at the receiver; therefore, it is just not feasible to perform optimization for each channel use. We can use (11) to select the best solution of $\mathbf{H}_c$ from a discrete set of possible solutions. In our evaluation of the algorithm, we will be working with simple realization of $\mathbf{H}_c$ that limits the space to $\mathbf{H}_c \in \{\mathbf{H}_{1,2}\mathbf{B}_2, \mathbf{H}_{1,3}\mathbf{B}_3\}$. The constitution of $\mathbf{D}_2$ and $\mathbf{D}_2$ changes depending on the chosen $\mathbf{H}_c$. For example, if we choose $\mathbf{H}_c = \mathbf{H}_{1,2}\mathbf{B}_2$, then $\mathbf{D}_2 = \mathbf{I}$ and $\mathbf{D}_3 = \mathbf{H}_c^{\dagger}\mathbf{H}_{1,3}\mathbf{B}_3$. Conversely, if we choose $\mathbf{H}_c = \mathbf{H}_{1,3}\mathbf{B}_3$, then $\mathbf{D}_2 = \mathbf{H}_c^{\dagger}\mathbf{H}_{1,2}\mathbf{B}_2$ and $\mathbf{D}_3 = \mathbf{I}$.

IV. Pseudo-Lattice Treatment: Performance Analysis

Here, we find an upper bound for the probability of error of the proposed technique. The effective noise $\mathbf{n}_i$ denoted earlier is not necessarily Gaussian, and as a result, the analysis becomes nontrivial. The probability of error can be represented by the probability that $\mathbf{n}_i$ does not fall within the Voronoi region of $\mathbf{0}$ as follows:

$$\begin{aligned}P_e &= \Pr\left[\varphi(\mathbf{n}_i) \neq 0\right] = \Pr\left[\mathbf{n}_i \notin \mathcal{V}_\Lambda(\mathbf{0})\right]\\ \Pr\left[\mathbf{n}_i \notin \mathcal{V}_\Lambda(\mathbf{0})\right] &= \Pr\left[\|\mathbf{n}_i\|^2 \geq \|\mathbf{n}_i - \boldsymbol{\lambda}\|^2,\ \forall\boldsymbol{\lambda}\in\mathbf{\Lambda}\right]\\ &= \Pr\left[\mathrm{Re}\{\boldsymbol{\lambda}^H\mathbf{n}_i\} \geq \|\boldsymbol{\lambda}\|^2/2,\ \forall\boldsymbol{\lambda}\in\mathbf{\Lambda}\right].\end{aligned} \tag{12}$$

By applying the Chernoff bound, we get for any $\nu > 0$

$$\Pr\left[\mathbf{n}_i \notin \mathcal{V}_\Lambda(\mathbf{0})\right] \leq \sum_{\boldsymbol{\lambda}\in\mathbf{\Lambda}}\mathbb{E}\left\{e^{\nu\mathrm{Re}\{\boldsymbol{\lambda}^H\mathbf{n}_i\}}\right\}e^{-\nu\|\boldsymbol{\lambda}\|^2/2}. \tag{13}$$

To overcome the analysis complexity, we will assume that the shaping region of the higher dimension lattice $\mathbf{\Lambda} = \mathcal{L}([\mathbf{H}_{i,i}\mathbf{H}_c])$ is a rotated hypercube in the complex domain $\mathbb{C}^N$, i.e., the Voronoi region of $\mathbf{\Lambda}$ can be denoted as follows:

$$\mathcal{V}(\mathbf{\Lambda}) = \gamma \mathbf{U}\mathcal{H} \tag{14}$$

where $\gamma > 0$ is a scalar, $\mathbf{U}$ is a unitary matrix, and $\mathcal{H}$ is a unit hypercube in $\mathbb{C}^N$. The assumption of hypercube shaping [11] simplifies the performance analysis; however, there is no shaping gain from the unshaped rectangular grid lattice [12], [13].

Under this assumption, the probability in (13) becomes

$$\Pr\left[\mathbf{n}_i \notin \mathcal{V}_\Lambda(\mathbf{0})\right] \leq \sum_{\boldsymbol{\lambda}\in\mathbf{\Lambda}} e^{\frac{\nu^2\|\boldsymbol{\lambda}\|^2\sigma_z^2 + \sum_{j=2}^{3}\left\|\nu\boldsymbol{\lambda}\left(\mathbf{H}_c(\mathbf{D}_j - \varphi(\mathbf{D}_j))\right)\right\|_F^2 P_s/4}{4}} e^{-\nu\|\boldsymbol{\lambda}\|^2/2}. \tag{15}$$

If we choose $\nu = 1/(\sigma_z^2 + P_s\sum_{j=2}^{3}\|\mathbf{H}_c(\mathbf{D}_j - \varphi(\mathbf{D}_j)\|_F^2)$, we simplify the expression to

$$\Pr\left[\mathbf{n}_i \notin \mathcal{V}_\Lambda(\mathbf{0})\right] \leq \sum_{\boldsymbol{\lambda}\in\mathbf{\Lambda}} e^{-\frac{d^2(\mathbf{\Lambda})}{4\left(\sigma_z^2 + P_s E_\varphi\right)}} \tag{16}$$

where

$$E_\varphi = \left\| \sum_{j=2}^{3} \mathbf{H}_c\left(\mathbf{D}_j - \varphi(\mathbf{D}_j)\right) \right\|_F^2.$$

The probability that $\mathbf{n}_i$ is not in the Voronoi region of $\mathbf{0}$ is approximately equal to the probability of the point being in the Voronoi region of the closest neighbor point to zero. Therefore, (16) can be approximated to

$$P_e \leq \mathcal{K}(\mathbf{\Lambda}) \exp\left(-\frac{d^2(\mathbf{\Lambda})}{4\left(\sigma_z^2 + P_s E_\varphi\right)}\right) \tag{17}$$

where $d(\mathbf{\Lambda})$ is the minimum distance between the two lattice points in $\mathbf{\Lambda}$ as follows:

$$d(\mathbf{\Lambda}) = \min\left\{\|\boldsymbol{\lambda}_1 - \boldsymbol{\lambda}_2\|_2 | (\boldsymbol{\lambda}_1, \boldsymbol{\lambda}_2) \in \mathbf{\Lambda}, \boldsymbol{\lambda}_1 \neq \boldsymbol{\lambda}_2\right\}$$

and $\mathcal{K}(\mathbf{\Lambda})$ represents the number of directions where the distance is the minimum $d(\mathbf{\Lambda})$. For the received lattice $\mathbf{\Lambda} = \mathcal{L}([\mathbf{H}_{i,i}\mathbf{H}_c])$, the minimum distance represents the minimum ℓ_2-norm of the columns of matrix $[\mathbf{H}_{i,i}\mathbf{H}_c]$.

For interference alignment, it is worth noting that, at receiver i, we are interested in correct decoding of the desired signal only. Therefore, in our performance analysis, we will focus on the detection error for signals in the desired signal subspace. We define a new parameter, i.e., $d_1(\mathbf{\Lambda})$, as the minimum distance along the lattice basis where the desired signal changes. $d_1(\mathbf{\Lambda})$ can be discerned from $\mathbf{H}_{i,i}$. The columns of the matrix $\mathbf{H}_{i,i}$ represent the directions in which the desired signal component of the lattice changes, as shown in Fig. 2. We can therefore denote $d_1(\mathbf{\Lambda})$ as the minimum ℓ_2-norm of the columns of $\mathbf{H}_{i,i}$. Expression (17) can now be written as

$$P_e \leq \mathcal{K}(\mathbf{\Lambda}) \exp\left(-\frac{d_1^2(\mathbf{\Lambda})}{4\left(\sigma_z^2 + P_s E_\varphi\right)}\right). \tag{18}$$

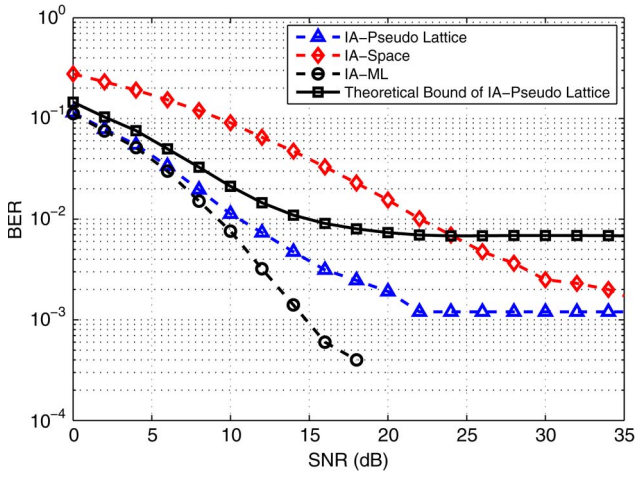

Fig. 3. BER versus SNR for the pseudo-lattice decoder with S-IA precoders. QPSK modulation number of antennas $N = 4$ and the channel variance $\sigma_h^2 = 1$.

A. Performance Bound

The performance of the decoder in (18) depends on the tuple $\{\mathbf{H}_c, \mathbf{D}_2, \mathbf{D}_3\}$ and the SNR condition of the channel. In low-SNR conditions, the effective noise at the receiver is dominated by the background noise. Therefore, P_e in (18) is upper bounded by

$$P_e \leq \mathcal{K}(\mathbf{\Lambda}) \exp\left(-\frac{d_1^2(\mathbf{\Lambda})}{4\sigma_z^2}\right). \tag{19}$$

Expression (19) is the performance of the ML receiver in an AWGN channel.

In high-SNR conditions, the effective noise is bounded by the channel approximation noise. Therefore, expression (18) can be upper bounded in high-SNR conditions as

$$P_e \leq \mathcal{K}(\mathbf{\Lambda}) \exp\left(-\frac{d_1^2(\mathbf{\Lambda})}{4\,P_s\,E_\varphi}\right). \tag{20}$$

The expression (20) shows that the performance of the system experiences an error floor as SNR increases. This can be seen through the simulations in the following section.

V. Simulation Results

Here, we present Monte Carlo simulations that were carried out to verify our proposed technique. A three-user interference network is simulated and it is assumed that the elements of the interference channels $\mathbf{H}_{i,j}$ are i.i.d. with circularly symmetric complex Gaussian distribution with zero mean and unity variance. The power used at each of the transmitters is unity, i.e., $P_s = 1$.

In Fig. 3, we compare the performance of our pseudo-lattice decoder at user 1 with the ZF receiver used in [5] and ML decoder in terms of bit error rate (BER). ML decoding is performed as

$$\tilde{\mathbf{w}}_\mathbf{1}: \min_{\tilde{\mathbf{w}}_\mathbf{1},\tilde{\mathbf{w}}_\mathbf{2},\tilde{\mathbf{w}}_\mathbf{3}} \|\mathbf{r}_1 - (\mathbf{H}_{1,1}\mathbf{B}_1\tilde{\mathbf{w}}_\mathbf{1} + \mathbf{H}_{1,2}\mathbf{B}_2\tilde{\mathbf{w}}_\mathbf{2} + \mathbf{H}_{1,3}\mathbf{B}_3\tilde{\mathbf{w}}_\mathbf{3})\|^2. \tag{21}$$

The number of antennas per user is $N = 4$ and QPSK modulation is used. Matrix $\mathbf{H}_c$ is chosen such that $\mathbf{H}_c \in \{\mathbf{H}_{1,2}\mathbf{B}_2, \mathbf{H}_{1,3}\mathbf{B}_3\}$ and $\mathbf{D}_j = \mathbf{H}_c^\dagger \mathbf{H}_{1,j}\mathbf{B}_j$. The choice of $\mathbf{H}_c$ is based on which of the two realizations minimizes (11). Fig. 3 also includes the theoretical bound for BER based on Section IV to verify our simulations results. From the figure, we can observe that the proposed pseudo-lattice decoder provides better performance for S-IA than the receiver used in [5]

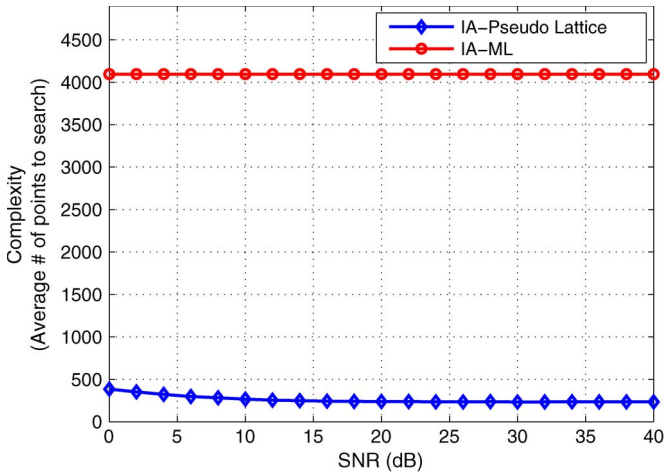

Fig. 4. BER versus SNR for the pseudo-lattice decoder with S-IA precoders. QPSK modulation number of antennas $N = 4$ and the channel variance $\sigma_h^2 = 1$.

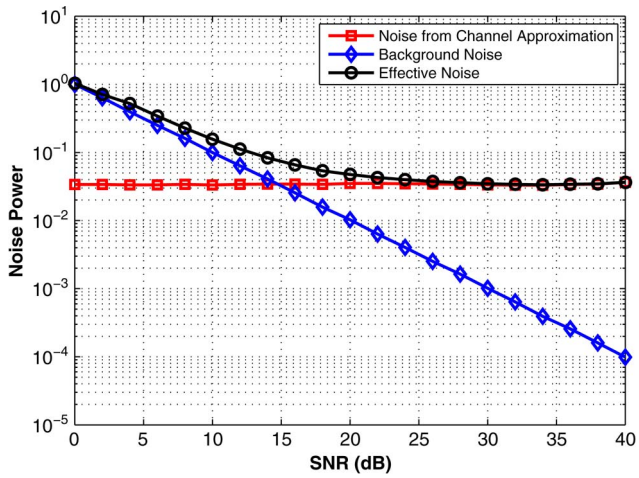

Fig. 5. Effective noise at user 1 (n_1) versus SNR for the pseudo-lattice decoder with S-IA precoders. QPSK modulation number of antennas $N = 4$, and the channel variance $\sigma_h^2 = 1$.

and [14] in low- and medium-SNR conditions. The performance of our pseudo-lattice decoder is close to the ML decoder exhibiting a difference of less than 1 dB in low-SNR conditions. The pseudo-lattice decoder approximates a common basis for the interference subspace such that the entire signal space can now fit into a lattice structure. Although this provides substantial gains in performance in low-SNR conditions, the approximation noise becomes more significant as the SNR improves. Therefore, Fig. 3 shows an error floor in high SNR ranges for the pseudo-lattice decoder.

Fig. 4 shows the difference between the search space for our technique versus the search space for ML decoders. ML decoders perform an exhaustive search over all possible vectors in the signal space. Therefore, ML decoders search through $(4^2)^3$ combinations.[1] In the pseudo-lattice decoder, the signal has a lattice structure after our treatment; therefore, we use a sphere decoder to decode the desired signal. It is observed from the figure that the number of points searched to arrive at a decoding decision is less than 10% of the search for ML.

[1]We have four constellation points in QPSK and a message of size 2 is transmitted from each of the three users.

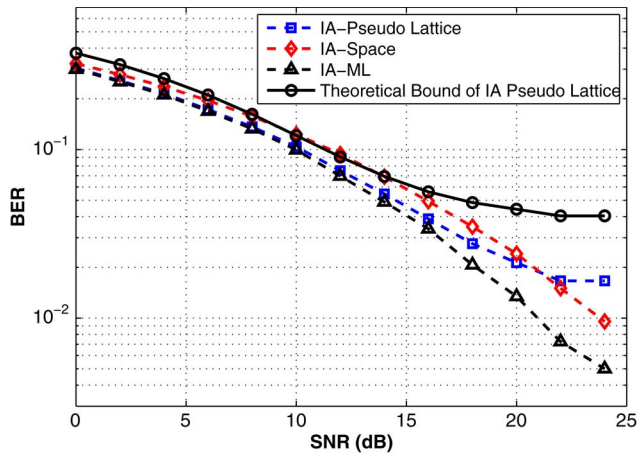

Fig. 6. BER versus SNR for the pseudo-lattice decoder with S-IA precoders. The 16-QAM number of antennas $N = 2$ and the channel variance $\sigma_h^2 = 1$.

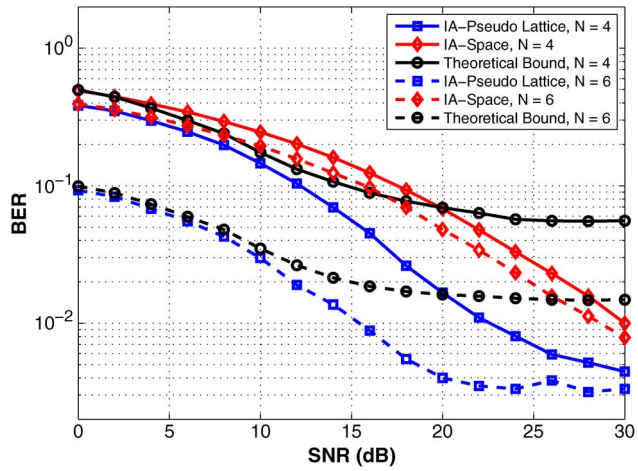

Fig. 7. BER versus SNR for the pseudo-lattice decoder with S-IA precoders. The 16-QAM modulation number of antennas $N = 4$ and 6, and the channel variance $\sigma_h^2 = 1$.

Fig. 5 shows the change of different components of the effective noise $\mathbf{n}_1$ with SNR. From the figure, we can observe that, at low-SNR conditions, the major noise source is the background noise. This can be shown by the effective noise tracing the background noise component in low-SNR conditions. Since the channel approximation noise is dependent on the channel variances, the noise exhibits a flat energy value over different SNR conditions. In higher SNR, background noise falls below the channel approximation noise, and the effective noise power asymptotically traces the channel approximation noise.

Figs. 6 and 7 show the BER when the simulation repeated using 16-QAM for $N = 2, 4, 6$. We note that, for the scenarios with $N = 4, 6$, the ML performance is not included as the search would have to go through $(16^2)^3$ and $(16^3)^3$ combinations, respectively. We note that the performance of the pseudo-lattice decoder is better than the ZF decoder in low- and medium-SNR ranges. As the number of antennas increases, the gain from applying our technique becomes more evident as can be perceived by comparing the two figures.

VI. Conclusion

We have proposed a pseudo-lattice decoding that enables LR-based decoding for S-IA in low and medium SNR ranges. Our proposed

technique can be also used for L-IA in all SNR ranges. Our discussion has shown that this approach can be applied by a user in a three-user network for all users while not disrupting S-IA or L-IA at the other two users. Using simulations, we have compared the performance of the proposed decoder with the ML decoder and the ZF decoder for S-IA. With lower complexity, as compared with the ML decoder, our decoder is shown to perform better than the ZF decoder and close to the performance of the ML decoder for low and medium SNR ranges. In high SNR conditions, an error floor is noted.

REFERENCES

[1] V. R. Cadambe and S. A. Jafar, "Interference alignment and spatial degrees of freedom for the k user interference channel," in *Proc. IEEE ICC*, 2008, pp. 971–975.

[2] K. Gomadam, V. R. Cadambe, and S. A. Jafar, "Approaching the capacity of wireless networks through distributed interference alignment," in *Proc. IEEE GLOBECOM*, 2008, pp. 1–6.

[3] G. Bresler, A. Parekh, and D. N. Tse, "The approximate capacity of the many-to-one and one-to-many Gaussian interference channels," *IEEE Trans. Inf. Theory*, vol. 56, no. 9, pp. 4566–4592, Sep. 2010.

[4] S. Sridharan, A. Jafarian, S. Vishwanath, S. A. Jafar, and S. Shamai, "A layered lattice coding scheme for a class of three user Gaussian interference channels," in *Proc. 46th Annu. Conf. Allerton Conf. Commun., Control, Comput.*, 2008, pp. 531–538.

[5] J. Choi, "Interference alignment over lattices for mimo interference channels," *IEEE Commun. Lett.*, vol. 15, no. 4, pp. 374–376, Apr. 2011.

[6] H. Yao and G. W. Wornell, "Lattice-reduction-aided detectors for mimo communication systems," in *Proc. IEEE GLOBECOM*, 2002, vol. 1, pp. 424–428.

[7] D. Wubben, R. Bohnke, V. Kuhn, and K.-D. Kammeyer, "Near-maximum-likelihood detection of MIMO systems using MMSE-based lattice reduction," in *Proc. IEEE Int. Conf. Commun.*, 2004, vol. 2, pp. 798–802.

[8] B. Nazer and M. Gastpar, "Compute-and-forward: Harnessing interference through structured codes," *IEEE Trans. Inf. Theory*, vol. 57, no. 10, pp. 6463–6486, Oct. 2011.

[9] V. Ntranos, V. R. Cadambe, B. Nazer, and G. Caire, "Integer-forcing interference alignment," in *Proc. IEEE ISIT*, 2013, pp. 574–578.

[10] C. Feng, D. Silva, and F. R. Kschischang, "An algebraic approach to physical-layer network coding," in *Proc. IEEE ISIT*, 2010, pp. 1017–1021.

[11] O. Shalvi, N. Sommer, and M. Feder, "Signal codes," in *Proc. IEEE Inf. Theory Workshop*, 2003, pp. 332–336.

[12] G. D. Forney, Jr., "Multidimensional constellations. II. Voronoi constellations," *IEEE J. Sel. Areas Commun.*, vol. 7, no. 6, pp. 941–958, Aug. 1989.

[13] N. Sommer, M. Feder, and O. Shalvi, "Shaping methods for low-density lattice codes," in *Proc. IEEE ITW*, 2009, pp. 238–242.

[14] H. Sung, S.-H. Park, K.-J. Lee, and I. Lee, "Linear precoder designs for k-user interference channels," *IEEE Trans. Wireless Commun.*, vol. 9, no. 1, pp. 291–301, Jan. 2010.

A Reconfigurable Digital Receiver for Transmitted Reference Pulse Cluster UWB Communications

Yongnu Jin, Hongwu Liu, *Member, IEEE*, Kyeong Jin Kim, *Senior Member, IEEE*, and Kyung Sup Kwak, *Member, IEEE*

***Abstract*—The transmitted reference pulse cluster (TRPC) structure for ultrawide bandwidth communications contains compactly spaced reference and data pulses and enables the use of a robust autocorrelation detector at the receiver. Since the digital receiver not only can avoid the problems caused by using the analog autocorrelation but can provide flexibility in its signal processing at the expense of high sampling rate of an analog-to-digital converter (ADC) as well, we consider the digital architecture for the recently proposed TRPC signaling scheme and propose a reconfigurable TRPC (rec-TRPC) receiver. The received signal-to-noise ratio (SNR) can be maximized in the new designed receiver by using the optimum number of delay line (DL) branches. The performance of the rec-TRPC receiver is analyzed, and our semi-analytical and simulation results show that the rec-TRPC receiver structure achieves up to a 2-dB power gain over the original TRPC receiver. Furthermore, the complexity of the rec-TRPC receiver is investigated from an implementation viewpoint and compared with the digital implementation of the original TRPC receiver.**

***Index Terms*—Delay line (DL), noncoherent receiver, transmitted reference pulse cluster (TRPC), ultrawide bandwidth (UWB).**

I. INTRODUCTION

The transmitted reference (TR) technique has been extensively studied for ultrawide bandwidth (UWB) communications since it has simple implementation and robust performance [1]. The basic idea of the TR scheme is to transmit a reference and data signal pair separated in time [2]. To avoid interpulse interference (IPI), the delay time between the reference pulse and information-bearing pulse must be larger than the length of the channel impulse response, which ranges from 50 ns to more than 100 ns for a typical UWB system [3]. This implies a relatively low data rate of TR. Moreover, [4] and [5] indicate that implementing accurate wideband delay lines (DLs) longer than 10 ns is unacceptable for practical analog UWB systems. To address this challenging long-wideband-DL problem, a frequency multiplexed TR in [6], a frequency-shifted reference scheme in [7], and a dual-pulse (DP) scheme in [8] and [9] were developed. In [10], a new TR pulse cluster (TRPC) system was proposed, and the integration interval determination methods for the TRPC system were further investigated in [11]. The TRPC structure not only provides the best performance among the aforementioned TR signaling schemes but enables

Manuscript received March 16, 2012; revised March 6, 2013, October 1, 2013, and February 24, 2014; accepted February 27, 2014. Date of publication March 24, 2014; date of current version November 6, 2014. This work was supported by the Ministry of Education Science and Technology of the Government of Korea under Grant 2010-0018116. The review of this paper was coordinated by Dr. X. Dong.

Y. Jin, H. Liu, and K. S. Kwak are with Inha University, Incheon 402-751, Korea (e-mail: grape412@163.com; hongwu.liu@ieee.org; kskwak@inha.ac.kr).

K. J. Kim was with Inha University, Incheon 402-751, Korea. He is now with Mitsubishi Electric Research Laboratories, Cambridge, MA 02139 USA (e-mail: kyeong.j.kim@hotmail.com).

Color versions of one or more of the figures in this paper are available online at http://ieeexplore.ieee.org.

Digital Object Identifier 10.1109/TVT.2014.2313337